Clean Technol., Vol. 30, No. 3, September 2024, pp. 211-219

청정생산공정기술 보 문

Improvement of the Surface Roughness of a 3D Stereolithographic Part for a Molded Interconnect Device

Jeong Beom Ko, Hyeon Beom Kim, and Young Jin Yang*

Korea Institute of Industrial Technology
102 Jejudaehak-ro, Jeju-si 63243, South Korea

(Received for review July 25, 2024; Revision received August 7, 2024; Accepted August 7, 2024)

Abstract

3D printing technology has created a paradigm shift in industries by achieving breakthrough innovations and enabling the fabrication of complex products. However, 3D printed parts are inferior in terms of their strength and surface quality compared to parts fabricated by conventional manufacturing methods. This study aims to improve the surface roughness of stereolithographic parts by experimental analysis of the generated area error. A photocurable polymer material was used for fabrication, and the effect of important parameters, such as the material viscosity, printing speed, pneumatic pressure, UV intensity, and pattern spacing, on the surface roughness were analyzed. The results showed that a high-viscosity (12,000 cP) thixotropic material formed a constant pattern with an aspect ratio of 1:1, and the pattern shape was maintained after printing. A pattern with a minimum thickness of 145 μm was formed at a printing speed of 70 mm/s and a pneumatic pressure of 20 kPa. These parameters were found to be suitable for low surface roughness. A UV laser at an intensity of 10 ~ 30 mW/cm^2 was used to form a smooth surface at low curing intensities. Moreover, it was seen that with a pattern spacing of 110 ~ 130 μm, a stereolithographic part with a low surface roughness of Ra 1.29 μm could be fabricated.

Keywords : Additive manufacturing, 3D printing, Direct cure, Direct printing, Surface roughness, Area error, UV intensity, Pattern spacing

1. Introduction

3D printing is a technology in which the digital drawing information designed or modeled in 3D is input to a 3D printer to obtain the output in three-dimensional form. It is a core technology that is changing the existing industrial paradigm and bringing breakthrough innovations to the manufacturing industry, while supporting a new market for creative economy. However, the final products obtained by 3D printing generally exhibit inferior quality in terms of the strength, durability, surface roughness, and level of finish and completeness compared to products fabricated by conventional manufacturing methods[1,2].

Recently, a variety of researches have being actively done in order to improve the surface roughness of the stereolithographic parts produced by 3D printing. For instance, 3D printing technology with a photocurable resin and fused deposition modeling (FDM) technology using filament materials are mainly used for the above-mentioned problem[3-6].

Kim et al.[7] investigated the optimal temperature to improve the surface quality of stereolithographic parts by minimizing the shrinkage rate of the unit curing line of photocurable resin unit, by controlling the temperature. For this purpose, an optimal temperature condition was computed through the analysis of the curing characteristics variation with the change in temperature.

Ahn et al.[8,9] developed a system to automatically select the molding direction and conducted research to improve the surface roughness of stereolithography parts by reducing the post-processing time. Kim et al.[10] developed a beam-projector-based PSLA(projection stereolithography) 3D printer that controls the size of the image formed on the tank by controlling the light source in order achieve the improvement in the dimensional accuracy of the stereolithographic parts.

As can be seen from the literature study, research is being conducted to improve the accuracy and surface roughness of 3D printed parts in various ways, but these characteristics are still regarded as the limitations of the 3D printing technology.

*To whom correspondence should be addressed.
E-mail: yangyj23@kitech.re.kr, Tel: +82-64-754-1533, Fax: +82-64-754-1520
https://doi.org/10.7464/ksct.2024.30.3.211 pISSN 1598-9712 eISSN 2288-0690

The 3D printing technology that fabricates a 3D stereolithographic part by curing only the photocurable resin has the advantages of producing the 3D parts with a higher strength, and not requiring any post-processing as compared to the conventional method[11]. MID manufacturing technology using this technology is much lighter and more sophisticated than other materials, and it can produce smaller or more diverse devices compared to other manufacturing methods.

In this study, the main process parameters of 3D printing, based on the photocurable polymer materials, were analyzed, and thus optimum process conditions were derived in order to improve the surface roughness of the stereolithographic parts. Furthermore, we investigated the method of improving the surface accuracy of stereolithographic parts by obtaining a curing condition that minimizes the area error generated between the layers using the filling up characteristics of the material.

2. Material and methods

2.1 Materials and characterization

In this study, photocurable material (Model: SE-8272, Fotopolymer Pte. Ltd.) and spot UV (Model: LSH20562, Liim tech Co., Ltd.) were used.

The typical UV-curable polymers can be categorized into low-viscosity (about 500 cP or less), medium-viscosity (about 500 ~ 10,000 cP) and high-viscosity (about 10,000 cP or more) materials. Amongst these, the used in our 3D printing process is a high-viscosity thixotropic material. Which shows the property of molecules agglomerating after being dispensed. Thus, the material does not spread during printing and can form a set pattern, which serves as an advantage in stacking stereolithography parts.

Manufactured stereolithography part was observed by a digital microscope (AM7115MZTL, Dino-Lite, Taiwan) and optical microscope (BX60M, OLYMPUS, JAPAN). The surface roughness analysis of stereolithographic parts was done using 3D profiler (NV-2400, NANOSYSTEM, KOREA). The resistivity of the electrode pattern was evaluated using a semiconductor device analyzer (B1500A, KEYSIGHT, USA).

2.1.1 Photocuring mechanism

When a UV-curable polymer is exposed to UV light, the photoinitiators present in the material absorbs the UV energy to generate radicals or cations to initiate polymerization. Thus, an instantaneous polymerization reaction takes place between the monomers and oligomers, the main components of the material. In particular, the polymerization reaction is caused by the crosslinking of the monomers, oligomers and photoinitiators, and the reaction time of crosslinking is determined by the total amount of energy that the polymer material is exposed to the UV light. Accordingly, the degree of UV curing can be controlled, which can help in improving the surface roughness of the stereolithographic parts [12,13].

2.2 Printing process

2.2.1 Dispensing mechanism

Figure 1 is a schematic diagram of the dispensing mechanism of a micronozzle, is the radius of the nozzle entrance, and equation 1 gives the relationship among the material supply flow rate (Q), printing speed (V), and the radius of the nozzle exit (R_d). As evident from Equation (1), when the material supply flow rate is constant, the dispensing mechanism can be used for control, and it can be estimated as a function of the printing speed. In this way, it can be seen that the pattern thickness can be controlled by the exit radius of the nozzle, which determines the accuracy of the printed stereolithographic part[14,15].

$$Q = \alpha \times \pi R_{\mathrm{d}}^2 \times V \tag{1}$$

2.2.2 Dispensing meniscus

In order to fabricate a part by 3D stereolithography, the thickness and line width of the pattern to be printed should be kept constant, and for this, a meniscus should be formed by the dispensing flow rate among the nozzle exit, the printing bed, and the printing speed [16].

Figure 2 shows the diagram of the meniscus shape. The experiment was conducted under changing conditions in the range of printing speed 40 mm/s to 70 mm/s and dispensing flow rate 20 kPa to 60 kPa. When the dispensing flow rate is excessively increased as compared to the printing speed, the pattern unfolds and leaks as shown in Figure 2(a), and irregular pattern widths are formed. On the contrary, when the flow rate decreases, the pattern breaks, as shown in Figure 2(c). In this case, the remaining amount of material that has not been transferred from the nozzle exit to the substrate accumulates, and when it is exposed to the UV curing equipment, the curing occurs from the tip of the nozzle, resulting in the clogging of the nozzle. Therefore, the dispensing flow rate

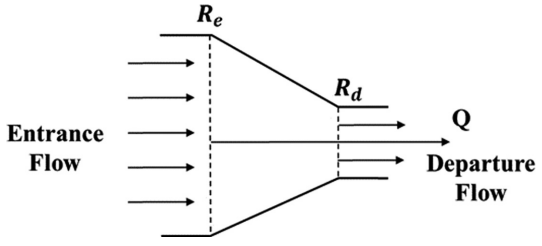

Figure 1. Schematic diagram of the dispensing mechanism of micronozzle.

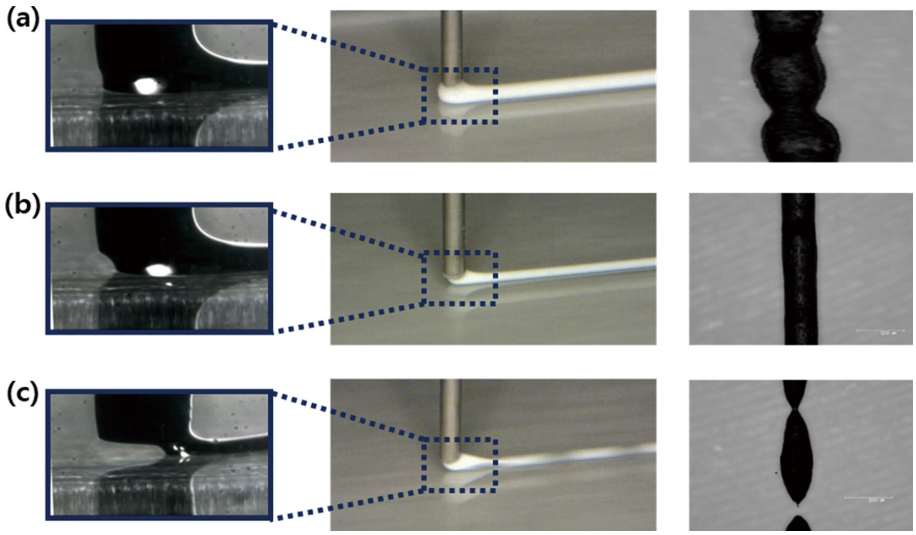

Figure 2. Meniscus change according to printing speed and dispensing flow rate. (a) If the dispensing flow rate is too high for the printing speed, a set pattern cannot be produced, as it starts leaking. (b) Optimum balance between printing speed and dispensing flow rate is achieved, forming meniscus and producing a set pattern. (c) The pattern breaks owing to insufficient dispensing flow rate for the printing speed.

and printing speed are variables in a trade-off relationship, and the steady state condition of meniscus can be maintained through their optimization, as shown in Figure 2(b)[17].

2.3 Correlation analysis of variables

2.3.1 UV curing mechanism

The total amount of energy (W), which the UV-curable polymers are exposed to, is shown in Figure 3, and it is controlled by the perpendicular height (H) of the UV lens and nozzle exit, the lateral distance (D) between the nozzle exit and UV lens, the distance (A) from the UV lens to the nozzle exit, the UV glancing angle (θ), and UV intensity (P).

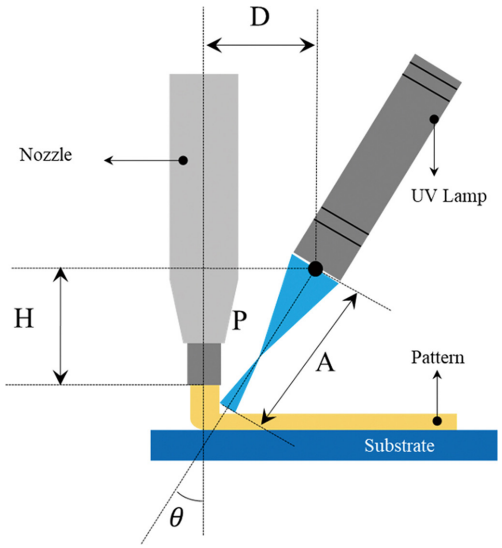

Figure 3. UV cure mechanism analysis.

The total amount of energy produced by the UV laser increases or decreases depending on the distance between the UV lens and nozzle exit. In particular, as the distance gets reduced, the total amount of energy increases, leading to a corresponding increase in the crosslinking reaction time. In addition, as the UV intensity increases, the total amount of energy increases. If the UV intensity decreases, the crosslinking reaction (among monomers, oligomers, and photoinitiators) is delayed. This results in the material being filled up in the liquid state, thereby reducing the area error produced between the layers of the stereolithographic part[18].

The total amount of energy (W) (generated by the UV laser) that the UV-curable polymers are exposed to can be represented in Equation (2) below. The lateral distance between the nozzle exit and the UV lens (D) is expressed in Equation (3). Using the angle (θ) between the nozzle and the UV curing equipment, the distance from the UV lens to the nozzle exit (A) can be expressed in Equation (4), and the consequent total amount of energy is defined in Equation (5). In other words, the amount of energy that the UV curable polymer materials are exposed to depends on the UV intensity and the distance from the UV lens to the nozzle tip[18,19].

$$W = \frac{P}{A} \tag{2}$$

$$D = H \cdot \tan\theta \tag{3}$$

$$A = \frac{D}{\sin\theta} = \frac{H \cdot \tan\theta}{\sin\theta} \tag{4}$$

$$W = \frac{P \cdot \sin\theta}{H \cdot \tan\theta} \tag{5}$$

2.3.2 The area error method

The area error here refers to the area error of the edge that appears when the stereolithographic part is cut into a vertical section, and the error arises from the difference between the layers constituting the stereolithographic part. As given in Figure 4, it can be seen that the surface roughness of the stereolithographic part becomes lesser, with the decrease in the area error[19,20].

The area error can be represented in an equation, using the height (H), glancing angle (θ), pattern thickness (t), and number of layers (n). The pattern thickness acts as a major determinant in area error. The area error of one layer on the surface is equal to the area of the right triangle between the horizontal layer and the inclined plane. Accordingly, the base of the right triangle can be obtained as in Equation (6), and the area error A_e is as in Equation (7). Here, to obtain the total area error, multiplying by the number of layers "n" can be expressed as in Equation (8). In theory, if glancing angle becomes "0", the error becomes "0" and the surface roughness can also become "0", but this is impossible in a realistic process.

In this study, a method of partially curing the material to fill the area error range was used to reduce the area error. This partial cure is possible by adjusting the amount of UV energy[12,13].

$$H = \frac{1}{\tan\theta} \cdot t \tag{6}$$

$$A_e = \frac{1}{2} \cdot t \cdot H = \frac{t^2}{2\tan\theta} \tag{7}$$

$$A_t = \frac{1}{2} \cdot t^2 \cdot \frac{1}{\tan\theta} \cdot n \tag{8}$$

3. Results and discussion

3.1 Pattern analysis using different material viscosities

In the fabrication of the stereolithographic part, the control of its surface roughness becomes easier when the printing aspect ratio is closer to 1:1, while maintaining the meniscus during the material dispensing. In order to analyze the printing pattern, a patterning

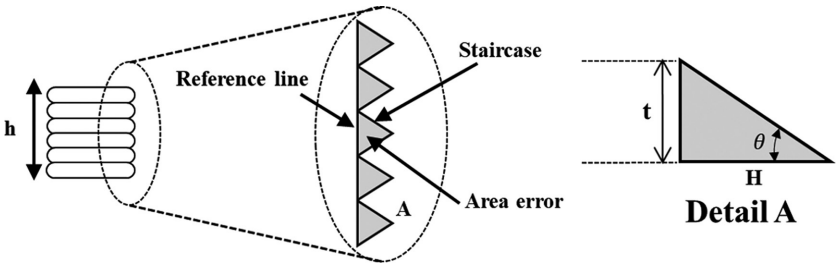

Figure 4. Theoretical numerical analysis of area error.

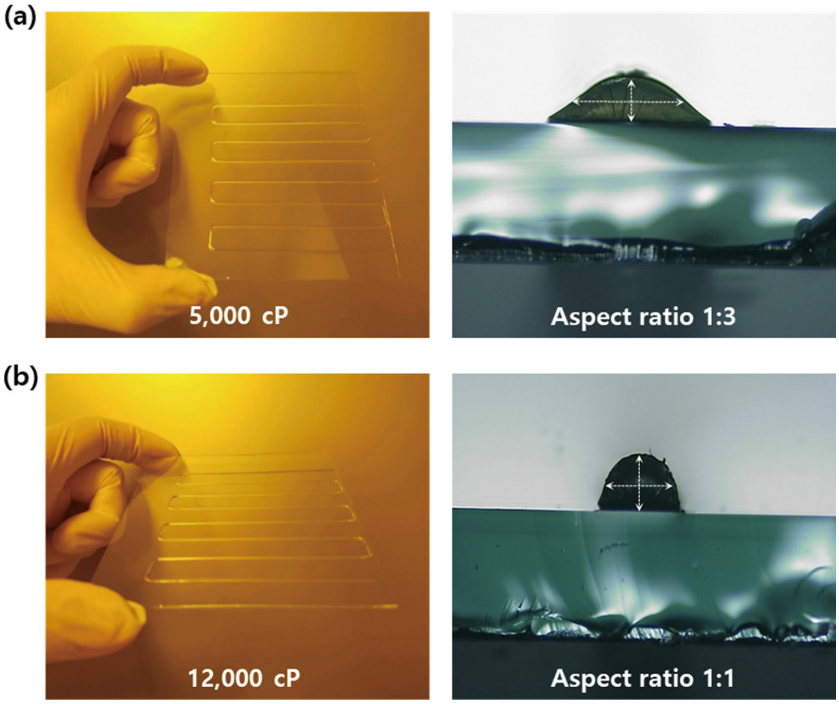

Figure 5. Pattern shape analysis by material viscosity.

experiment was conducted using materials with three types of viscosities: low (500 cP), medium (5,000 cP), and high (12,000 cP).

Figure 5 shows the pattern shape analysis results for different material viscosities. It is seen that the pattern shape is not formed when the low-viscosity material is used. On the contrary, a pattern with an aspect ratio 1:3 is formed in the case of the medium-viscosity material. The high-viscosity thixotropic material formed a constant pattern with an aspect ratio 1:1, and the pattern shape was maintained after printing.

3.2 Printing speed and output pneumatic pressure for printing

The surface roughness of the stereolithographic part is determined by the pattern thickness. As the pneumatic pressure increases under constant printing speeds, the dispensed amount of the material increases, thereby increasing the pattern thickness. With the conditions summarized in Table 1, the pattern thickness is analyzed according to the printing speed, and pneumatic pressure conditions. As can be seen from the graph in Figure 6, a pattern with a minimum thickness of 145 μm was formed when a printing speed of 70 mm/s and a pneumatic pressure of 20 kPa was used. Moreover, a pattern with the maximum thickness of 250 μm was formed under the conditions of a printing speed of 40 mm/s and a pneumatic pressure of 60 kPa.

Table 1. Printing speed and pneumatic pressure conditions for pattern thickness control

Nozzle size	400 μm
UV intensity	30 mW/cm^2
Stand-off distance	200 μm
Pneumatic	20 ~ 60 kPa
Printing speed	40 ~ 70 mm/s

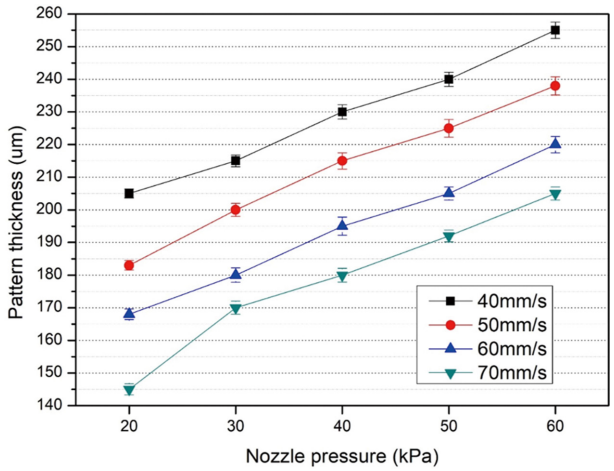

Figure 6. Pattern thickness variation, according to printing speed and pneumatic pressure conditions.

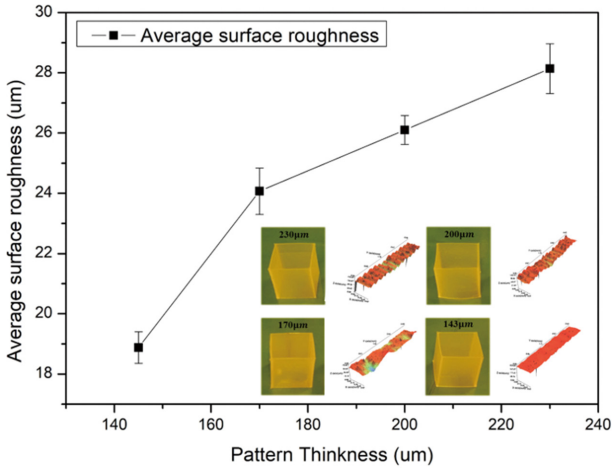

Figure 7. Average surface roughness of the 3D shape of the tetrahedral stereolithographic part.

In order to examine the change in the surface roughness of the stereolithographic part, according to the changes in printing speed and pneumatic pressure conditions, a tetrahedral stereolithographic part of 20 mm^3 was fabricated. A three-dimensional nano-shape measuring system (model: WT-250, procured from Nanosystemz. Co. Ltd.) was used to measure the surface roughness of the specimen (having dimensions of 1 mm width and 3 mm length) at four different locations in the X-axis direction, at 0.2 mm intervals.

As for the average surface roughness, which is shown in Figure 7, the resolution increased with the decrease in pattern thickness, and it was confirmed that the surface resolution of the stereolithographic part can be improved by controlling the conditions of printing speed and pneumatic pressure.

3.3 UV output intensity

Another process parameter that can improve the surface roughness of the stereolithography part is the UV intensity, and the change in surface roughness was analyzed by varying the UV intensity 5 ~ 30 mW/cm^2. At an intensity of 5 mW/cm^2, it was seen that the total amount of energy was not sufficient enough to enable any crosslinking reaction, and thus the material was not cured. Thereby, the printing pattern collapsed, making it impossible to fabricate the stereolithographic part.

In order to examine the surface accuracy of the tetrahedral stereolithographic part at a UV intensity ranges of 10 ~ 30 mW/cm^2, the surface roughness of the stereolithography part was measured at three different locations (at a interval of 0.3 mm) in a sample area of 1 mm width and 3 mm length, having 4 faces in total, starting from the directions of the width in x direction. The measurements were achieved using a 3D nano-shape measurement system. As a result of the analysis shown in Figure 8, the surface accuracy error for the respective stereolithographic parts were

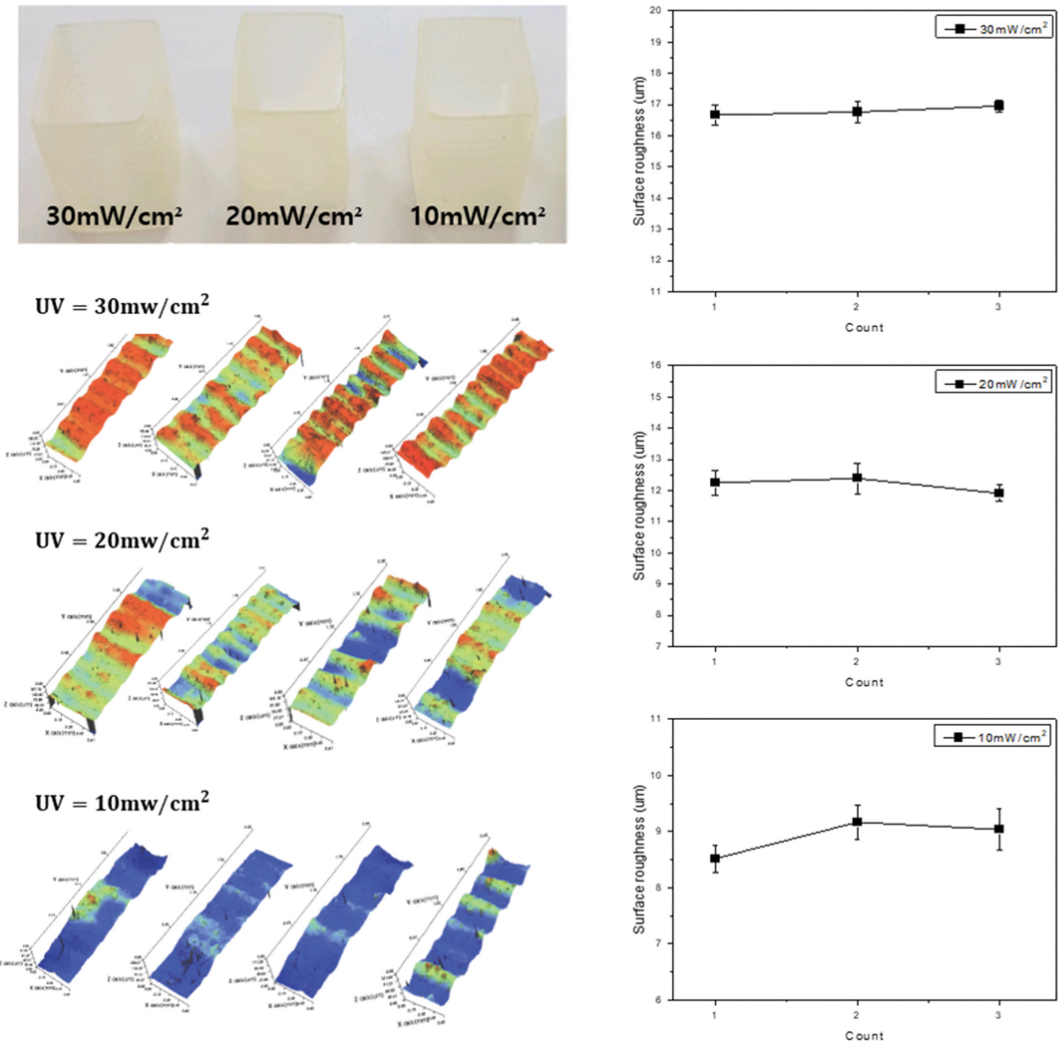

Figure 8. Analysis of the surface roughness variation of stereolithographic parts, according to UV intensity.

approximately equal to 1.1 ~ 1.8 μm, confirming an excellent surface accuracy.

When the UV intensity was 10 mW/cm^2, the surface was found to be smoothest with the average surface roughness of all the faces of the tetrahedral part being Ra 8.9 μm and the average standard deviation is Ra 0.22 μm. This is attributed to the fact that as the UV intensity is lower, the crosslinking reaction time of the monomers, oligomers, and photoinitiator is increased, leading to the incomplete curing and consequently the material's leaking into the region of area error between the layers.

3.4 Pattern spacing

The pattern line width and proper pattern spacing are important factors that determine the effectivity of the fabrication, and the surface roughness of stereolithographic parts. Accordingly, the stereolithography part stacking experiment was conducted by increasing the spacing from 110 μm to 170 μm at 20 μm interval.

Figure 9 shows the experimental results according to the pattern line width and pattern spacing. This incomplete consumption signified that some material remained at the nozzle tip or dispensed material lacked. With the pattern spacing of 150 ~ 170 μm, the pattern line width and spacing were not properly balanced, resulting in large area errors and low-accuracy products.

As for the stereolithographic parts, fabricated with spacing 110 μm and 130 μm, the line width and spacing were optimally balanced with each other, enabling the fabrication of the stacked structure. As shown in Figure 9, the average surface roughness (Ra) were 1.95 μm and 1.29 μm, respectively in 4 measurement areas, confirming a quite high accuracy.

3.5 Fabrication of Electrode pattern

The effect of improving the surface roughness of stereolithography parts means that it can be applied to MID (Mold Interconnect Device) manufacturing technology. MID technology is a component manufacturing method that forms a three-dimensional circuit/electrode pattern on the surface of a molded product. This technology

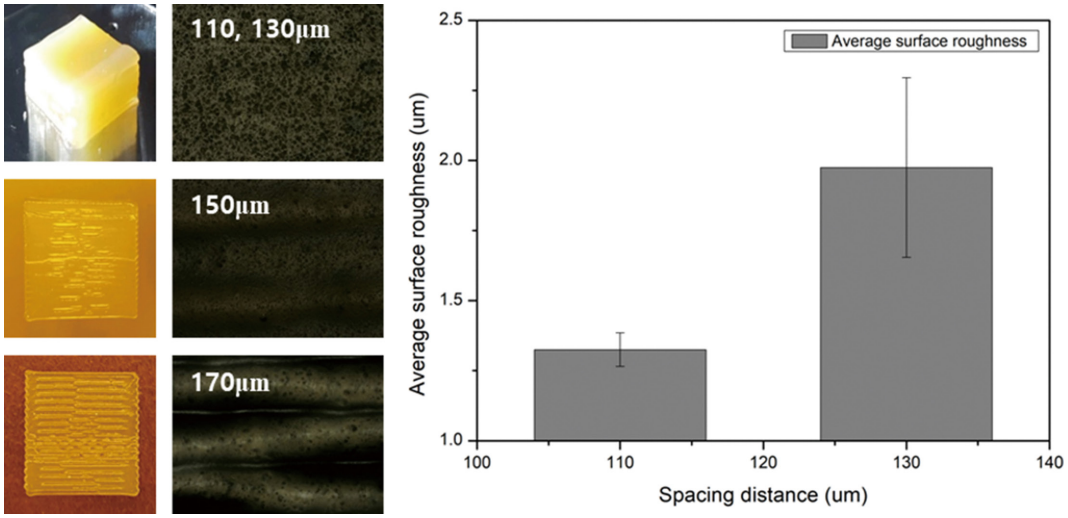

Figure 9. Analysis of surface roughness according to dispensing pattern spacing.

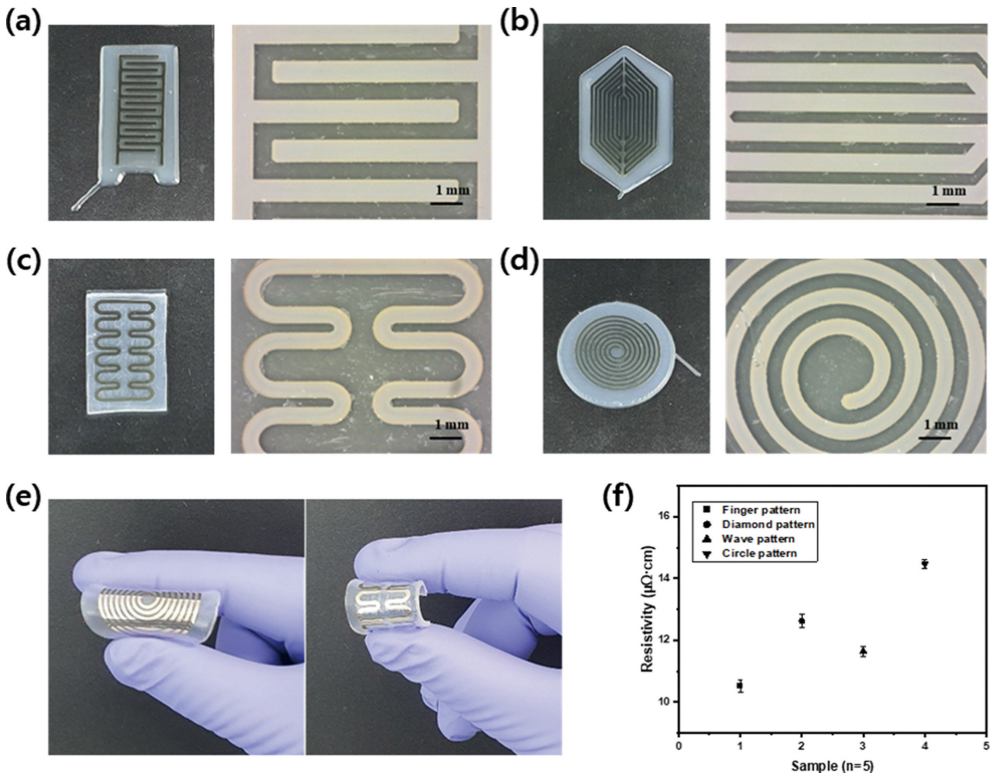

Figure 10. Result images of electrode pattern for various shapes on the surface of stereolithography part. (a) Finger pattern. (b) Diamond pattern. (c) wave pattern. (d) Circle pattern. (e) Electrode pattern on flexible urethane substrates. (f) Resistivity results of different pattern shapes in molded interconnect device (n = 5, value = mean ± sd).

not only efficiently utilizes internal space, but also enables weight reduction, high quality, and miniaturization of parts.MID technology using photocurable resin enables device fabrication using substrates with various characteristics. In order to verify the effect of the surface roughness improvement of the stereolithography part, an Ag metal circuit was printed on the surface of the part. Figure 10 is the result of forming functional electrode patterns of various shapes on the surface of the sculpture. In Figure 10(a ~ b), a finger pattern and a diamond pattern were formed on the surface by fabricating a hard sculpture using an epoxy-based photopolymer.

Figure 10 (c ~ e) shows the result of wave pattern and circle pattern formation, and it was confirmed that it can be used for manufacturing flexible PCB substrates and devices by using urethane-based materials. The electrical characteristics of the electrode pattern formed on the surface of the optical sculpture were shown as Figure 10(f) through five resistivity measurements.

In this time, the results of finger pattern (10.5 ± 0.2 μΩ·cm), diamond pattern (12.6 ± 0.21 μΩ·cm), wave pattern (11.6 ± 0.14 μΩ·cm), and circle pattern (14.4 ± 0.15 μΩ·cm) are shown. Such a pattern can be used for various electronic devices by satisfying the performance of the functional electrode.

4. Conclusions

In this study, the optimum condition of pattern aspect ratio = 1:1 was established through a pattern analysis with different material viscosities, and it was confirmed that the surface roughness of the stereolithography part can be improved through the control of the printing speed and output pneumatic pressure.

At this time, the effect of UV intensity on the surface roughness was studied. Results showed that, in the intensity range of 10 ~ 30 mW/cm^2, a tendency to form a smooth surface was observed at low curing intensities, as a result of the filling up effect. However, a UV intensity of 5 mW/cm^2, is not possibly sufficient to maintain the set form of the pattern.

In the fabrication of the stereolithography part, the pattern line width and the pattern spacing are important parameters for the improvement of the surface roughness, as well as the fabrication of the stereolithography part. It was seen that with a pattern spacing of 110 ~ 130 μm, the stereolithographic part with a superior surface roughness of 1.29 μm was fabricated.

With the increased use of 3D printers, this study on the improvement of the major drawback of the 3D printer, i.e., high surface roughness, will lead to the product quality improvement, and facilitate the production of new and innovative products with incorporation of other processes. In order to further enhance the usability of the 3D printing technology, continuous research on quality improvement of parts is necessary.

Acknowledgements

This study has been conducted with the support of the Korea Institute of Industrial Technology as “Development of elemental technology for implementing next-generation freeform display based on arbitrary surfaces (kitech UR-24-0027).”

References

1. Choi, J.-W. and Kim, H.-C., “3D Printing Technologies - A Review,” *Korean Soc. Manuf. Proc. Eng.*, **14**(3), 1-8 (2015).
2. Lopes, A., Navarrete, M., Medina, F., Palmer, J., MacDonald, E., and Wicker, R., “Expanding Rapid Prototyping for Electronic Systems Integration of Arbitrary Form,” *Solid Freeform Fab. Symp. Proc.*, **17**, 664-655 (2006).
3. Vignesh, R., Suganthan, R., and Prakasan, K., “Development of CAD Models from Sketches: A Case Study for Automotive Applications,” *IMechE*, **221**, 41-47 (2007).
4. Ko, H. J., Kim, H. C., and Yun, H. Y., “Study on Fabrication of 3D MID Cruise Control Switch,” *Korean Soc. Mech. Eng.*, 1796-1797 (2013).
5. Lee, I. H., Jang, S. H., Oh, S. T., Kim, M. K., Kim, H. C., and Cho, H. Y., “3-Dimensional Circuit Device Fabrication Technology Based on the 3-D Printing,” *Korean Soc. Mech. Eng.*, 1896-1900 (2015).
6. Paik, B. M., Lee, J. H., Shin, D. S., and Lee, K. S., “Development of Three Dimensions Laser Direct Patterning System,” *Korean Soc. Manuf. Tech. Eng.*, **21**(1), 116-122 (2012).
7. Kim, S. H., Lee, E. D., and Paik, I. H., “Progress of the Stereolithography Product’s Shape Accuracy by Temperature Control of the Resin,” *Korean Soc. Prec. Eng.*, 808-811 (2000).
8. Ahn, D.-K., Kim, H.-C., and Lee, S.-H., “Selection of Build Orientation for Reducing Surface Roughness with Stereolithography Parts,” *Korean Soc. Prec. Eng.*, 137-140 (2001).
9. Ahn, D. K., Song, J. I., Kwon, S. M., and Lee, S. H., “A Computation Methodology of Support Contact Area in Stereolithography,” *Korean Soc. Mech. Eng.*, 629-632 (2008).
10. Kim, Y.-H., Kim, K.-E., and Lee, C., “Accuracy Improvement of Output in Projection Stereolithography by Optimizing Projection Resolution,” *J. Korean Soc. Manuf. Tech. Eng.*, **24**(6), 710-717 (2015).
11. Jung, J., Huh, K. S., Jae, J., and Lee, K. S., “Fabrication and Characterization of Disposable Golf Tees using Biodegradable Polymer through 3D Printing,” *Clean Technol.*, **29**(3), 172-177 (2023).
12. Jun, J. U., Jung, J. S., Hwang, Y. M., Kim, S. K., Kim, J. A., Ke, J. Y., and Ha, M. K., “A Study on the Surface Roughness and Area Error at FDM,” *Korean Soc. Manuf. Tech. Eng.*, 24-29 (2002).
13. Jun, J. U., Kwon, H. J., Kim, S. K., Kim, J. A., Jung, J. S., and Ha, M. K., “Prediction of Sphere Surface by the Theoretical Area Error at FDM,” *Korean Soc. Prec. Eng.*, 262-265 (2002).
14. Heller, B. P., Smith, D. E., and Jack, D. A., “Effects of Extrudate Swell and Nozzle Geometry on Fiber Orientation in Fused Filament Fabrication Nozzle Flow,” *Additive Manuf.*, **12**, 252-264 (2016).
15. Lu, G., Wang, X.-D., and Duan, Y.-Y., “A Critical Review of Dynamic Wetting by Complex Fluids: From Newtonian Fluids to Non-Newtonian Fluids and Nanofluids,” *Adv. Coll. Inter. Sci.*, **236**, 43-62 (2016).
16. Gao, Q., Niu, X., Shao, L., and Zhou, L., “3D Printing of Complex GelMA-based Scaffolds with Nanoclay,” *Biofabrication*, **11**(3), 1-22 (2019).

17. Anantharamaiah, N., Tafreshi, H. V., and Pourdeyhimi, B., "Numerical Simulation of the Formation of Constricted Waterjets in Hydroentangling Nozzles: Effects of Nozzle Geometry," *Trans IChemE, Part A*, **84**(3), 231-238 (2006).
18. Vatani, M. and Choi, J.-W., "Direct-print Photopolymerization for 3D Printing," *Rapid Prototy. J.*, **23**(2), 337-343 (2017).
19. Garcia, E. A., Qureshi, A. J., and Ayranci, C., "A Study on Material-process Interaction and Optimization for VAT-photopolymerization Processes," *Rapid Prototy. J.*, **24**(9), 1479-1485 (2018).
20. Jun, J. U., Jung, J. S., Kim, S. K., Kim, J. A., Kwon, H. J., and Ha, M. K., "A Study on the Improvement in Surface Roughness of Rapid Prototype at FDM," *Korean Soc. Mech. Eng.*, 195-200 (2002).